Supplementary Information

A Liquid-Free Conducting Ionoelastomer for 3D Printable Multifunctional Self-Healing Electronic Skin with Tactile Sensing Capabilities

Qirui Wu, [a,b] Yidan Xu, [c] Songjiu Han, [a,b] Jundong Zhu, [a] Anbang Chen, [a] Jiayu Zhang, [a] Yujia Chen,[a] Xiaoxiang Yang, [b] Jianren Huang, [a,b,*] Lunhui Guan [a,d,*]

a. CAS Key Laboratory of Design and Assembly of Functional Nanostructures, Fujian Key Laboratory of Nanomaterials, Fujian Institute of Research on the Structure of Matter, Chinese Academy of Sciences, Fuzhou 350108, China.
b. School of Mechanical Engineering and Automation, Fuzhou University, Fuzhou 350108, China.
c. Department of Oncology, The First Affiliated Hospital of Anhui Medical University, Hefei 230000, China.
d. College of Chemistry, Fuzhou University, Fuzhou 350108, China.

†Electronic Supplementary Information (ESI) available.

See DOI: 10.1039/x0xx00000x

‡Authors with equal contributions.

KEYWORDS. 3D Printing, Tactile sensor, Electronic skin

Figure S1. The inks with and without tartrazine before photo-curing.

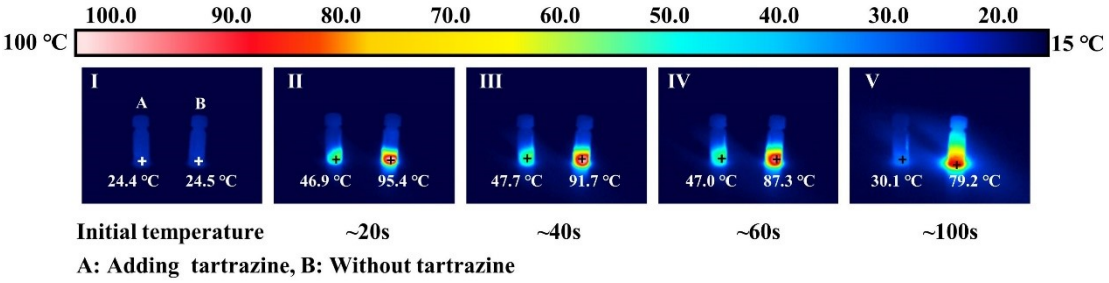

Figure S2. The effect of tartrazine on light curing exothermic heat of LFCIg was observed by thermal imaging

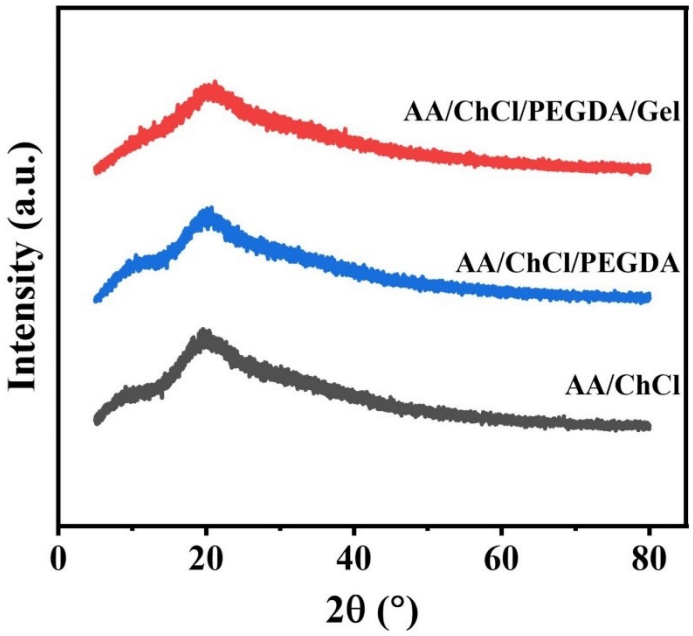

Figure S3. The XRD of different LFCIg components

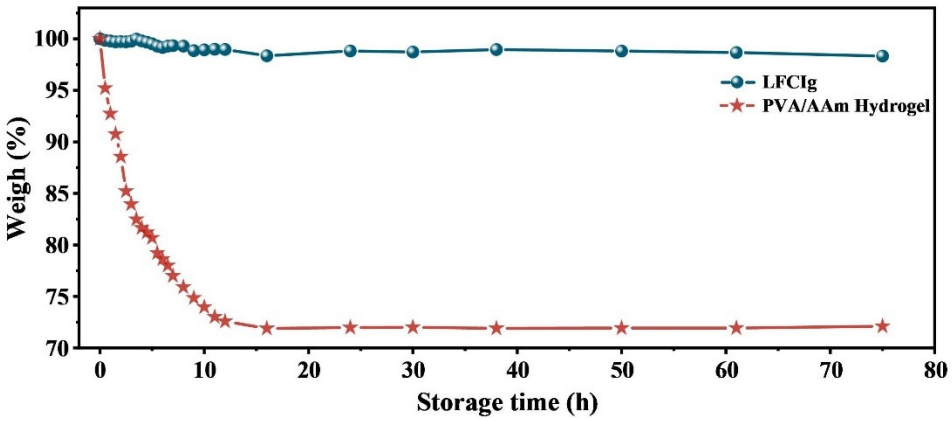

Figure S4. The LFCIg and PVA/AA hydrogels were stored at 80 ℃, while the material weigh changes were recorded continuously for 75 hours.

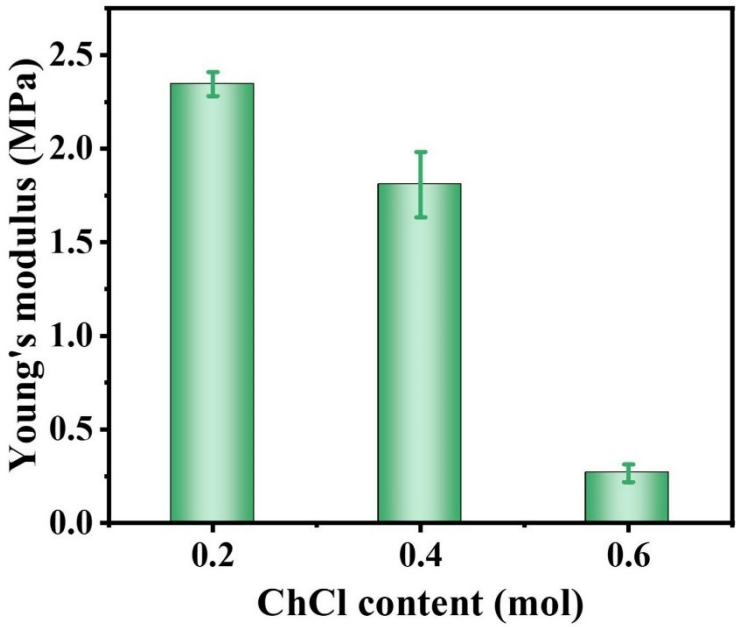

Figure S5. The Young's modulus of the LFCIg with different ChCl contents

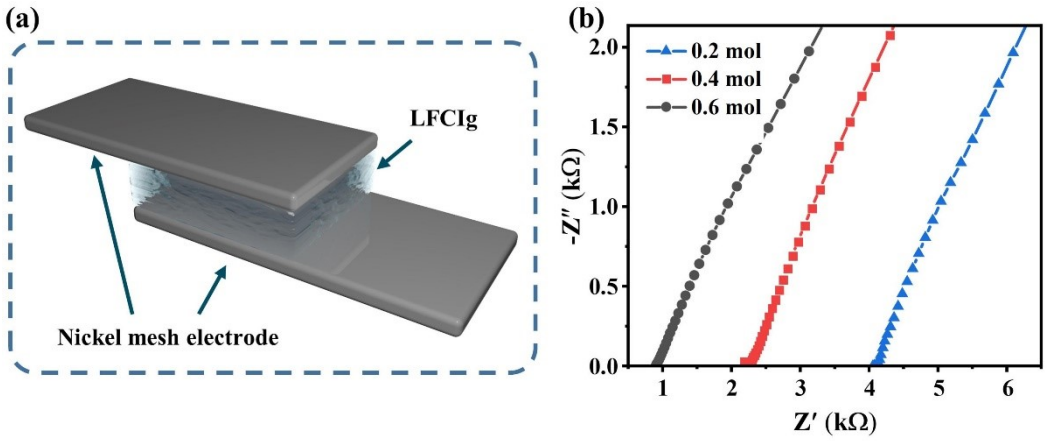

Figure S6. a) Schematic diagram of specimen assembly for LFCIg electrochemical test. b) Nyquist plot of LFCIg with different ChCl molar content.

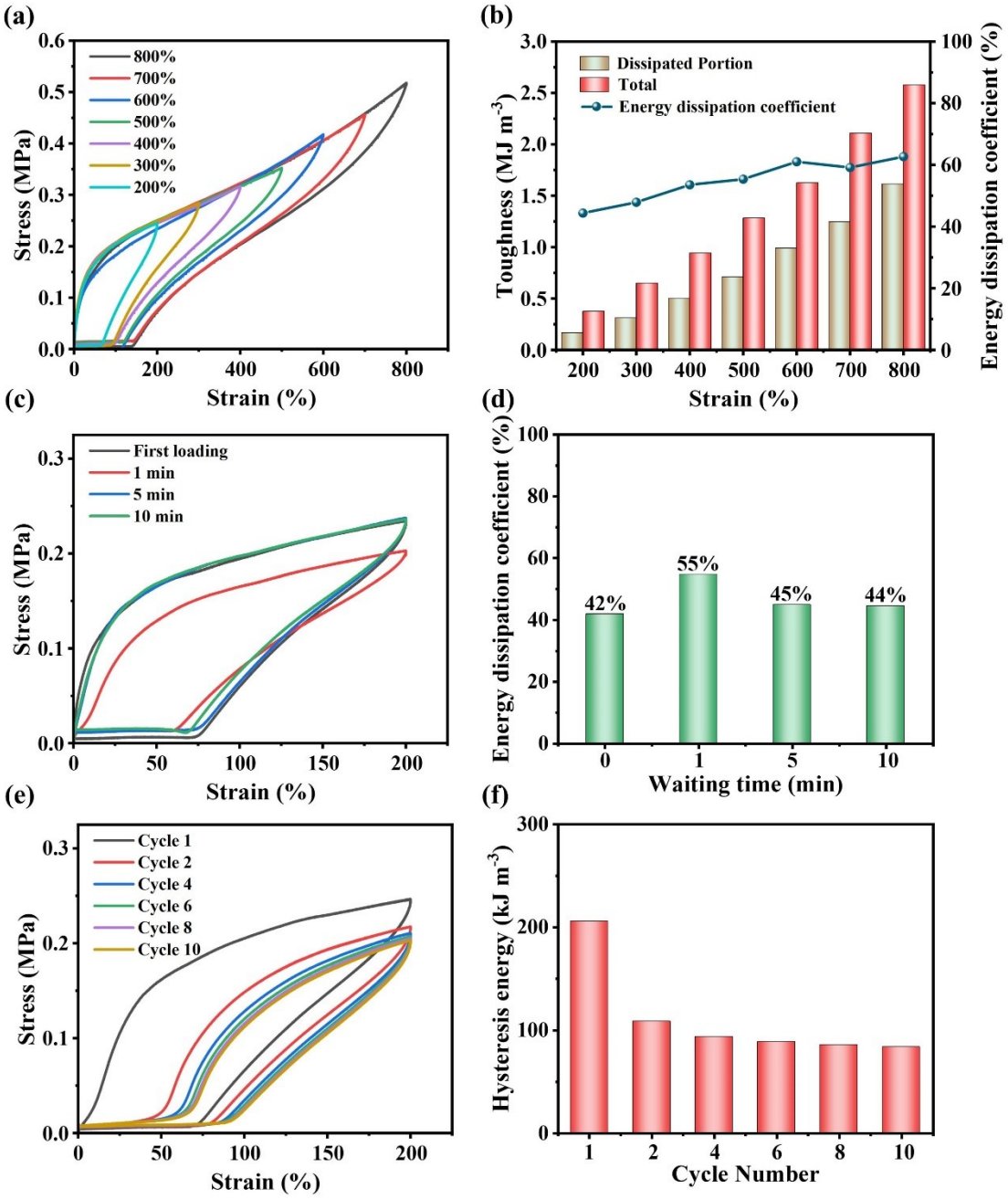

Figure S7. The LFCIg was subjected to a series of tensile cycling tests. a-b) Loading and unloading curves with strain ranges from 200% to 800% and corresponding toughness and energy dissipation coefficient. c-d) Cyclic loading-unloading curves at the 200% strain for different resting time between two consecutive tests and corresponding energy dissipation coefficient. e-f) Ten successive cyclic loading-unloading curves at 200% strain without resting time and corresponding hysteresis energy.

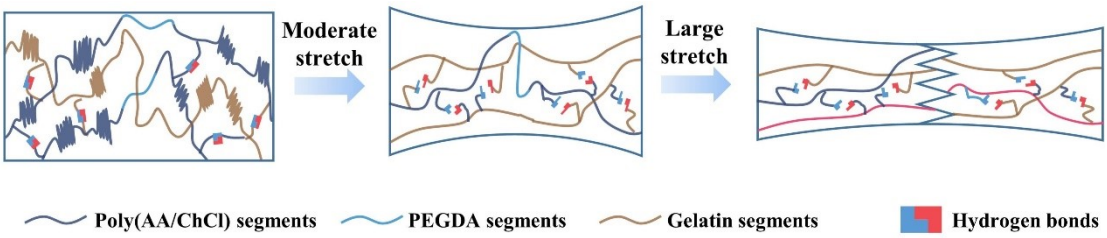

Figure S8. Schematic illustrations of the microstructure of the stretching sample.

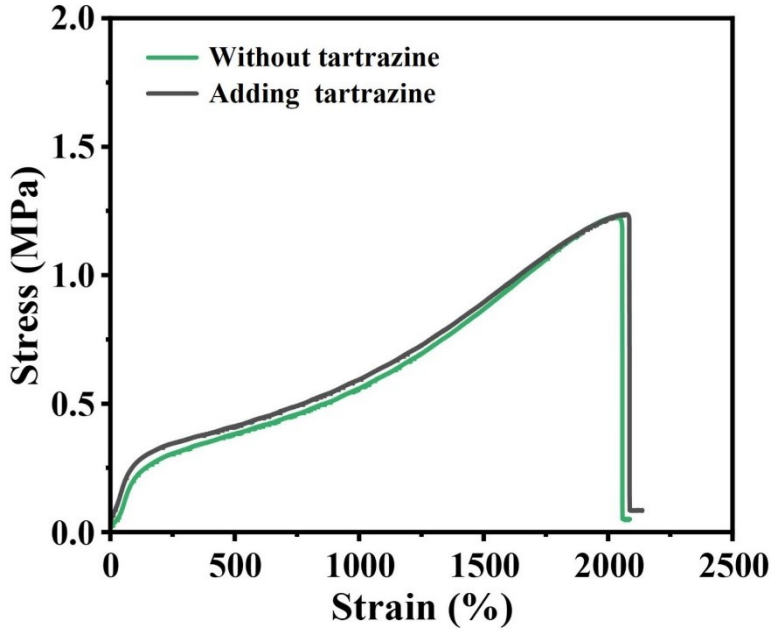

Figure S9. Mechanical tests with tartrazine and without tartrazine.

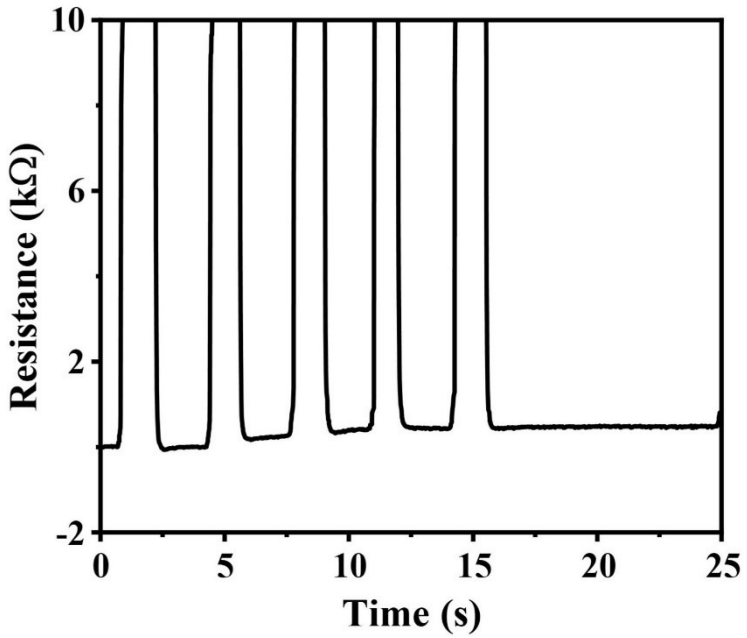

Figure S10. The self-healing process of LFCIg was observed by measuring its real-time resistance.

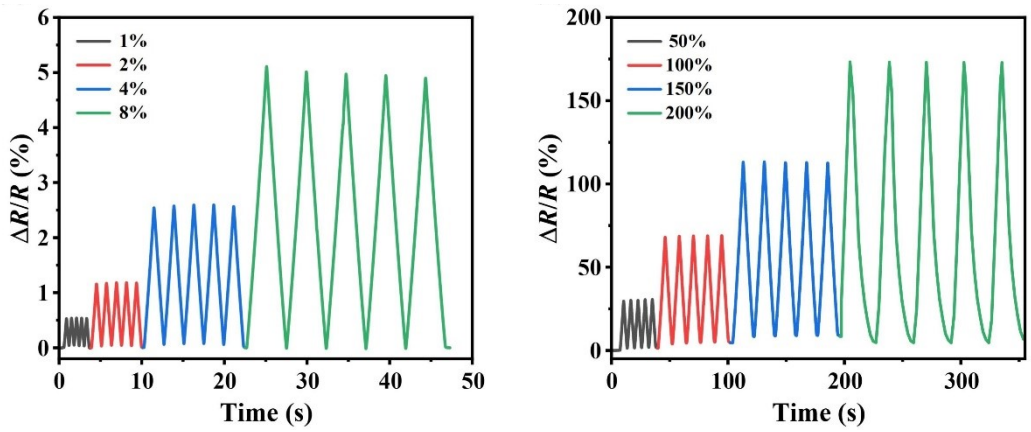

Figure S11. $\Delta R/R_0$ of SCIg sensor at small strain (1%~8%) and large strain (25%~200%).

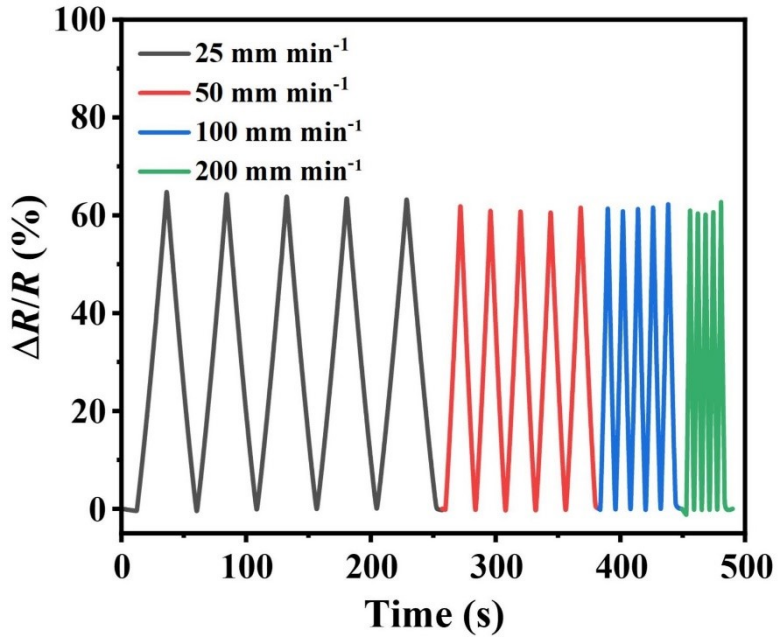

Figure S12. Relative resistance changes of SCIg when strain to 100% at different tensile rates.

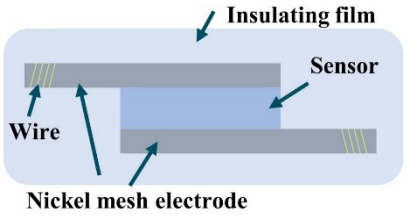

Figure S13. The single capacitive sensor was assembled by sandwiched between two electrodes with a 1×1 cm^2 ionogel

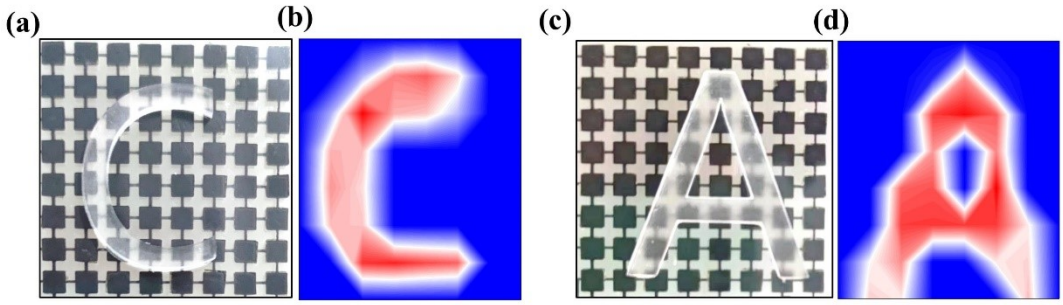

Figure S14. a-c) Optical images of the flexible large-scale e-skin with a C-shaped and A-shaped epoxy resin block on it, and b-d) the contour plot of 2D mapping.

Table S1. A rough comparison of conductivity and strain the between this work and recently reported typical ionic conductor materials

No.	Materials	Conductivity (mS m^{-1})	Strain (%)	Reference
1	**AA/ChCl/PEGDA/Gel**	23.3	2090	This work
2	**PTMEG/HEDS/LiTFSI Ionogel**	3.77	2615	[15] *Nat. Commun.* **2022**
3	**MEA/IBA/LiTFSI Ionogel**	5.28	1744	[21] *Adv. Mater.* **2021**
4	**PIL/[TFSI] Ionogel**	~13.1	540	[25] *Mater. Horiz.* **2020**
5	**AAm/MA/ChCl Ionogel**	~11	450	[44] *Chem. Mater.* **2020**
6	**BA/[EIC6A] [TFSI] Ionogel**	~4.17	1500	[47] *ACS Appl. Mater. Interfaces* **2021**
7	**HFBA/OEGA/Ils Ionogel**	~2.67	2000	[48] *ACS Appl. Mater. Interfaces* **2021**
8	**PAA/x-Ch ionogel**	5.15	1200	[49] *Adv. Funct. Mater.* **2021**
9	**PBA ICE**	1	1100	[50] *Nat. Commun.* **2018**
10	**LM-PDES elastomer**	13	2600	[51] *Adv. Funct. Mater.* **2021**
11	**PLA ICE**	2.4	800	[52] *J. Mater. Chem. A* **2021**
12	**PAA/betaine elastomer**	0.02	1600	[53] *Nat. Commun.* **2021**

Table S2. A rough comparison of recovery time and self-healing efficiency the between this work and recently reported typical ionic conductor materials

No.	Materials	Recovery time (s)	Self-healing efficiency (%)	Reference
1	**AA/ChCl/PEGDA/Gel**	0.16	90	This work
2	**PAA/ChCl/CMFs Ionogel**	~2.5	~100	[31] *Adv. Funct. Mater.* **2022**
3	**AAm/MA/ChCl Ionogel**	~0.6	~90	[44] *Chem. Mater.,* **2020**
4	**HFBA/OEGA/Ils Ionogel**	~0.8	~96.7	[48] *ACS Appl. Mater. Interfaces* **2021**
5	**PAM/PBA-IL/CNF hydrogel**	~10	~92	[54] *Adv. Funct. Mater.* **2022**
6	**PEG/PHEMA Ionogel**	2.8	~68	[55] *ACS Appl. Mater. Interfaces* **2022**
7	**BAA/ChCl/PDA@CNC**	0.5	~90	[56] *Chem. Mater.* **2022**
8	**PEDOT:PSS/PAAMPSA**	0.9	80	[57] *Adv. Mater.* **2022**
9	**TFEA/AAm/[EMIM][TFSI] Ionogel**	1.05	99	[58] *Adv. Mater.* **2021**
10	**Starch/PVA/Glycerol/$CaCl_2$**	1.2	100	[59] *J. Mater. Chem.A,* **2021**

Table S3. Mechanical properties and conductivity of LFCIg containing different mass fractions of ChCl

ChCl (mol)	Strain (%)	Stress (MPa)	Young's modulus (MPa)	Conductivity (mS m^{-1})
0.2	1305±45	4.73±0.05	2.35±0.06	5.66±0.10
0.4	1576±77	3.57±0.24	1.81±0.17	11.48±0.87
0.6	2100±50	1.23±0.01	0.27±0.05	23.27±2.47

Table S4. A rough comparison of sensitivity time and ultimate tensile strength the between this work and recently reported typical ionic conductor materials

No.	Materials	Sensitivity	Ultimate Tensile Strength (MPa)	Reference
1	**AA/ChCl/PEGDA/Gel**	3.54	4.76	This work
2	**P(MEA-co-IBA) elastomer**	2.2	1.05	[21] *Adv. Mater.* **2021**
3	**AA/ChCl/VAMCMCS**	1.183	3.2	[23] *Chem. Eng. J.* **2021**
4	**HFBA/OEGA/Ils Ionogel**	1	0.27	[48] *ACS Appl. Mater. Interfaces* **2021**
5	**PAA/x-Ch ionogel**	1	0.235	[49] *Adv. Funct. Mater.* **2021**
6	**LM-PDES elastomer**	2.17	0.125	[51] *Adv. Funct. Mater.* **2021**
7	**TFEA/AAm/[EMIM][TFSI] Ionogel**	1.85	0.72	[58] *Adv. Mater.* **2022**
8	**Starch/PVA/glycerol/$CaCl_2$**	3.4	0.6	[59] *J. Mater. Chem.A,* **2021**
9	**MEA/IBA/[C_2mim][NTf_2]**	~0.6	0.752	[60] *Adv. Funct. Mater.* **2021**
10	**[VBIm][BF4]/[C_{12}VIm][BF_4]**	0.5	1.1	[61] *Chem. Eng. J.* **2022**
11	**PAA/DMAPS/EMES**	2	1.06	[62] *Nat. Commun.* **2022**